# Sticking of Hydrogen Atoms to Crystalline Ice Surfaces: Dependence on Incidence Energy and Surface Temperature

**A. Al-Halabi,[†] A. W. Kleyn,[†] E. F. van Dishoeck,[‡] and G. J. Kroes*,[†]**

*Leiden Institute of Chemistry, Gorlaeus Laboratories, P.O. Box 9502, 2300 RA, Leiden, The Netherlands, and Leiden Observatory, P.O. Box 9513, 2300 RA Leiden, The Netherlands*

*Received: January 8, 2002; In Final Form: March 19, 2002*

We present results of classical trajectory calculations on the sticking of hydrogen atoms to the basal plane (0001) face of crystalline ice, $I_h$. The sticking probability is found to decrease with both incidence energy ($E_i$) and surface temperature ($T_s$). At the surface temperatures studied, the sticking probability can be fitted to a simple decay function: $P_s = 1.5\ e^{-E_i(K)/175}$ at $T_s = 10$ K, and $P_s = 0.85\ e^{-E_i(K)/175}$ at $T_s = 70$ K. In the trapped state, the adsorbed hydrogen atom is located on top of the ice surface, over the center of a surface hexagonal ring, interacting with all water molecules forming the ring. The calculated physisorption energy of the adsorbed atom is approximately $400 \pm 50$ K. The results of our calculations are compared with the experimental and theoretical data for amorphous ice surfaces. At $T_s = 10$ K, our values for the sticking probability are higher than those of Buch and Zhang [Buch, V.; Zhang, Q. *Astrophys. J.* **1991**, *379*, 647], which is attributed to differences in surface topology. Our sticking probability values are lower than those of Masuda et al. [Masuda, K.; Takahashi, J.; Mukai, T. *Astron. Astrophys.* **1998**, *330*, 243], which we attribute to an incorrect implementation of the H−$H_2O$ potential in their work. The experimental results available on hydrogen formation on amorphous ice are in good agreement with our results, if the assumption is made that all H-atoms that stick will recombine. Our calculations then suggest that the formation of $H_2$ through recombination of H-atoms adsorbed on the surface is efficient enough to compete with the cosmic destruction of $H_2$.

## 1. Introduction

The formation of molecules in the interstellar medium (ISM) is believed to occur via several channels.[1] One channel consists of gas-phase reactions, including radiative association of atoms and molecules. Another important channel consists of gas−surface reactions, which take place on dust particles.

In dense clouds, the dust-grain particles may have icy mantles consisting mainly of $H_2O$ and other molecules such as CO, $CO_2$, $NH_3$, and $CH_4$, which accumulate on the cores of the solid particles consisting of silicates and carbonaceous particles.[2] These icy mantles are believed to have an amorphous structure.[3] However, recent infrared experiments on silicate smokes (amorphous silicate particles of size 5−10 nm) showed that the water molecules condensed immediately in the crystalline form at low surface temperatures ($T_s \lesssim 20$ K).[4] On larger-sized amorphous silicate particles (micrometer), water initially condenses as amorphous ice at temperatures of interstellar interest. However, a phase transition of the deposited ice from the amorphous to the crystalline phase was found to occur above 110 K.[5] In the ISM, this phase transition can happen through impact of cosmic rays.

Recent experiments revealed a new, nonthermal, and indirect mechanism of UV-light-induced crystallization of monolayer and multilayer films of amorphous ice deposited on graphite at low surface temperatures ($T_s < 100$ K).[6] The experiments showed that the UV light photoexcites the electrons in the substrate, which in turn tunnel to defect states in the amorphous ice to induce exothermic crystallization. The results of these experiments may have an impact on the ideas concerning the structure of the ice surface in the ISM, in particular, for regimes in which UV photons penetrate, and studies on both amorphous and crystalline ice surfaces are needed.

Reactions on the surfaces of the dust grains have been suggested long ago to play an important role in the chemistry of the ISM and the formation of interstellar molecules.[7] Such reactions have been extensively studied over the last three decades, both experimentally[8−11] and theoretically.[12−27]

In the case of the formation of the most abundant molecule in the ISM, $H_2$, the radiative association of $H_{(g)} + H_{(g)}$ is too slow to compete with the photodissociation of $H_2$, because $H_2$ has no permanent dipole moment. In radiative association of $H_2$, the photon emitted upon recombination must result from the forbidden transition between the two Heitler−London states.[12] Other gas-phase reactions of hydrogen atoms with $H^+$ and $H^-$ to produce $H_2$ are likewise not sufficiently frequent to explain the observed abundance of $H_2$ in diffuse clouds, because of the low concentrations of $H^+$ and $H^-$.[28] It is therefore generally assumed that the source of $H_2$ is catalytic surface recombination of the hydrogen atoms, which can occur on grain surfaces.[15,16,28−31]

The hydrogen recombination may occur via one of two mechanisms: the Eley−Rideal (ER) mechanism[32,33] or the Langmuir−Hinshelwood (LH) mechanism.[34,35] In the first mechanism, a direct head-on collision occurs between an impinging hydrogen atom and an adsorbed atom on the surface, followed by desorption of a newly formed $H_2$ molecule, often in an excited rovibrational state. In the second mechanism, the adsorbed hydrogen atoms explore the surface adsorbing sites and eventually recombine and desorb (possibly in an excited state).[23] The two mechanisms described above involve the sticking and the accommodating of one or both of the hydrogen atoms to the grain surface. Also, the adsorbed atoms must reside at the surface for a long enough period of time for a head-on

[†] Leiden Institute of Chemistry.
[‡] Leiden Observatory.

10.1021/jp020007y CCC: $22.00 
Published on Web 05/31/2002

collision with an impinging hydrogen atom to occur (the ER mechanism), or to explore the sticking sites on the surface where other hydrogen atoms might be adsorbed (the LH mechanism). A high mobility of the adsorbed hydrogen atoms is necessary for the LH mechanism to be efficient. In this case, a sufficiently strong H−grain bond is necessary for adsorption to occur for a sufficiently long period of time, but the bond should not be so strong as to trap the adsorbed hydrogen atoms in localized states, which would hinder their mobility.[36]

Sticking of hydrogen atoms to the surfaces of icy mantles and the formation of molecular hydrogen have been investigated theoretically[12−23,25−27] and experimentally.[8−11] Theoretical studies have a long history starting 30 years ago, when Hollenbach and Salpeter performed quantum mechanical calculations to study the sticking of light gas atoms to surfaces.[14] The diffusion of an adsorbed atom on the surface was also studied.[14] Lennard-Jones potentials[37] were used to model the interaction between the impinging atom and the surface atoms. The surface was represented by a single harmonic oscillator characterized by a single driving frequency (the Debye frequency of the solid). The calculated sticking coefficient of the hydrogen atoms to ice was about 0.32 (for $T_s = 78$ K) and the calculated binding energy between 300 and 400 K.[14,15] The quantum hopping of the H-atoms that occurs at low surface temperatures (up to 10 K) was found to provide the mobility required for the adsorbed hydrogen atom to explore the adsorption sites. Hollenbach and Salpeter also briefly studied the formation of $H_2$ on ice. The calculations suggested that the newly formed $H_2$ molecule leaves the surface immediately upon the formation in high rotational and vibrational quantum states ($J = 8$ and $v = 12$, according to ref 14).

Various theoretical calculations have been performed after those pioneering studies to investigate the formation of $H_2$ on surfaces on the basis of macroscopic[16,23,38−40] and microscopic models.[22,25,27,41−44] In the macroscopic description of the $H_2$ formation, the rate equations of the hydrogen adsorption, desorption, and recombination are developed and solved. Recently, values of the parameters involved in the rate equations that best fit the experimental results[10,11,45] were implemented.[38−40] On the microscopic scale, molecular dynamics and quantum dynamics techniques were used to study the sticking, the hopping, and the recombination of the H-atoms on several surfaces that are relevant to the ISM, such as amorphous ice[22,25,42,43] and graphite.[26,27,41,44] The calculations showed that the newly formed $H_2$ has a significant amount of translational energy and is desorbed in rotationally and vibrationally excited states,[25,26,44] in qualitative agreement with the results of the calculations performed by Hollenbach and Salpeter.[14] The computed sticking probability of hydrogen to amorphous ice surfaces shows a strong dependence on incidence energy ($E_i$) and surface temperature ($T_s$).[22,42,44]

The results of recent beam experiments performed to study the molecular hydrogen formation on amorphous ice[46] showed a high formation yield of ∼0.4, even at low $T_s$ ($T_s = 10-12$ K). Those experimental results are in agreement with the results of the calculations of Hollenbach and Salpeter on sticking,[14] if one assumes unit probability that the adsorbed hydrogen atoms recombine,[11] in line with the Hollenbach and Salpeter model.[16] The experiments suggest that the hydrogen recombination observed in surface reactions on icy mantles is fast enough to compete with the cosmic ray destruction of $H_2$.

Formation of $H_2$ through surface recombination strongly depends on the nature of the surface. For the most part, this is due to differences in the dependence of the sticking of hydrogen on $T_s$ between different surfaces. For instance, beam experiments performed on a silicate surface made from a mixture of Mg−$SiO_3$ and Fe−$SiO_3$ showed that the sticking probability decreases very fast with $T_s$. As a result the formation yield of molecular hydrogen decreases by about an order of magnitude when $T_s$ increases from 4 to 10 K.[10,11] The measured recombination yield of molecular hydrogen from amorphous ice decreases much more slowly with $T_s$, because the sticking probability to amorphous ice depends less strongly on $T_s$ in the range $T_s = 4-20$ K.[46]

The previous classical trajectory (CT) calculations on sticking of hydrogen atoms to amorphous ice predicted different values for the sticking probability and the binding energies of the adsorbed atoms.[22,42] The calculations were performed on different surfaces but used the same H−$H_2O$ and $H_2O$−$H_2O$ interaction potentials. A small cluster of 115 water molecules was used by Buch and Zhang.[22] On the other hand, a periodic flat surface of 1000 water molecules was used by Masuda et al.[42] The crystalline ice surface, which can also be present in the ISM and play an important role in the formation of $H_2$, has not been considered yet. In this paper, we fill this gap by presenting results of CT calculations on sticking of hydrogen to the basal plane surface of crystalline ice, $I_h$. Our calculations also aim to clarify the large discrepancies between the previous results for amourphous ice.[22,42]

The paper is organized as follows. In section II, we present the method used in this study. The results are presented and discussed in section III and section IV, respectively. The astrophysical implications are also presented in section IV. The conclusions are offered in the last section.

## 2. Method

To study the sticking of hydrogen atoms to a crystalline ice surface, that is, the basal plane (0001) surface of ice $I_h$, the classical trajectory method was used.[47] We have essentially followed the same approach as used before to study the sticking of HCl to ice surfaces.[48,49]

**2.1. The Ice Surface.** The ice surface was simulated using the molecular dynamics (MD) method.[50] The surface was modeled using eight layers of moving water molecules, which were treated as rigid rotors but were otherwise allowed to move according to Newton's equations of motion. These mobile layers were superimposed on four layers of fixed water molecules. Periodic boundary conditions were applied in the directions parallel to the scattering surface (the $x$ and $y$ directions), to simulate an infinite ice surface. The MD box had replicated dimensions $x = 22.53$ Å and $y = 23.23$ Å and the thickness of the surface is 21.5 Å. The initial configuration of the surface obeyed the ice rules and had a zero dipole moment.[51] The MD surface contained 360 water molecules, of which 240 molecules were mobile. The TIP4P potential[52] was used to model the interaction between the water molecules. This potential was used because it yields stable hexagonal ice at higher temperatures (∼200 K)[53,54] and also at the range of temperatures relevant to this study, as verified in our simulations. Details on the model can be found in refs 48 and 53. The ice surface was equilibrated at the desired temperature, $T_s$ (10 or 70 K), using a computational analogue of a thermostat.[55] The thermostat was applied for about 1.0 ps, leaving the surface afterward to equilibrate for about 100 ps, using a time step of 1 fs, before the scattering trajectories were started. In the MD simulations and in the simulations of the collision dynamics discussed below, Newton's equations of motion of the hydrogen atom and the water molecules were integrated using an improved leapfrog algorithm developed by Fincham.[56]

**TABLE 1: The Parameters for the Pair Potential of Equation 2.1 Describing the H−$H_2O$ Interaction**

| *l,m* | $\epsilon_{l,m}$ [K] | $\sigma_{l,m}$ [Å] |
|---|---|---|
| 0,0 | 222.1 | 3.33 |
| 1,0 | −19.6 | 3.00 |
| 2,0 | 17.7 | 2.98 |
| 2,2 | 73.3 | 2.92 |

**2.2. The Impinging Hydrogen Atom.** In the classical trajectory calculations, the initial impact position and the angle of incidence of the impinging atom were selected at random, using the Monte Carlo technique.[47] The interaction potential between the hydrogen atom and the water molecule used here is the same pair potential as developed by Zhang et al.[57] and used to study the sticking of hydrogen and deuterium atoms to amorphous ice surfaces.[22] The pair potential used here is a fit of ab initio calculations on the $H_2O$−H system, using the unrestricted Hartree−Fock (UHF) with fourth-order Møller−Plesset perturbation theory (MP4).[57] The effect of the counterpoise correction for the basis set superposition error was also taken into account by using the method of Boys and Bernardi.[58] The $H_2O$−H potential has the form

$$V_{\mathrm{W-H}} = \sum_{l,m} 4\epsilon_{l,m}\left[\left(\frac{\sigma_{l,m}}{r}\right)^{12} - \left(\frac{\sigma_{l,m}}{r}\right)^{6}\right] Y_{l,m}(\theta,\varphi) = \sum_{l,m} \mathrm{LJ}_{l,m}(12-6) Y_{l,m}(\theta,\varphi) \quad (2.1)$$

In this potential, the origin is placed at the oxygen of the water molecule and the angles $\theta$ and $\varphi$ are the spherical angles of the impinging hydrogen atom with respect to a coordinate system in which the hydrogen atoms of the water molecule are at polar angles $\theta = 127.74°$ and $\varphi = \pm 90°$. The distance $r$ is the distance between the incident H-atom and the oxygen atom of the water molecule. The values that were used for the parameters occurring in the Lennard-Jones potentials $\mathrm{LJ}_{l,m}(12-6)$[37] are shown in Table 1.[22,57] The parameters $\epsilon_{l,m}$ in the $\mathrm{LJ}_{l,m}(12-6)$ potential were scaled by a factor of 1.43 to obtain good agreement with the experimental value of $\overline{\epsilon r}_{\min}$ for the spherically averaged LJ(12 − 6) potential of the $H_2O$−H system.[59] The experimental value of $\overline{\epsilon r}_{\min}$ was obtained by fitting to scattering data (integral cross sections) and has an estimated error of less than 10%. In the scattering experiments, only elastic scattering was considered.[59]

The calculations were performed for three different incidence energies, $E_i = 100$, 300, and 600 K, for two different surface temperatures, $T_s = 10$ and 70 K. For each set of conditions, 100 trajectories were calculated. Each trajectory was run for 6.7 ps, using a time step of 0.01 fs. It was necessary to use this small time step to avoid a drift in the total energy of the system, especially when the hydrogen atom is in the repulsive regime of the potential. The simulation period is sufficiently long to study the sticking of the impinging H-atom to the surface: the hydrogen atom reaches the first minimum of the distance to the surface (the first turning point of the *Z* coordinate of the hydrogen atom) within 2.5 ps of simulation (the exact time depending on the initial velocity and the angle of incidence). At the beginning of each trajectory, the impinging atom was placed at a distance of 10 Å above the ice surface. A continuous, well-behaved switching function was used to set the interaction potential of the $H_2O$−$H_2O$ molecules and the interaction of the $H_2O$−H to zero at a very long distance (≥10 Å).[48]

The ice surface was operationally defined to be at a height that is equal to $Z_s = 22.5$ Å (in the first monolayer, the upward pointing hydrogen atoms are at about 22.5 Å, while the oxygen atoms are at about 21.5 Å). A sticking trajectory was defined as a trajectory that exhibits more than one turning point in the *Z*-coordinate of the H-atom for motion normal to the surface, such that the final energy of the hydrogen atom being trapped either on top or inside of the ice surface is below −100 K.[22] Here, the energy of the hydrogen atom is the sum of the potential and the kinetic energy, where the zero of the potential energy is defined by the hydrogen atom being in the gas phase, that is, at a distance ≥10 Å from the ice surface. The other possibility is backscattering where the H-atom returns to the gas phase ($Z_f \geq 29.5$ Å). Some trajectories were run for an additional period of time to distinguish between these two types of trajectories. The sticking probability is defined as the number of the sticking trajectories divided by the total number of trajectories. Our definition of sticking probability is the same as that used by Masuda et al.[42] and that used by Buch and Zhang[22] for $S_E$.

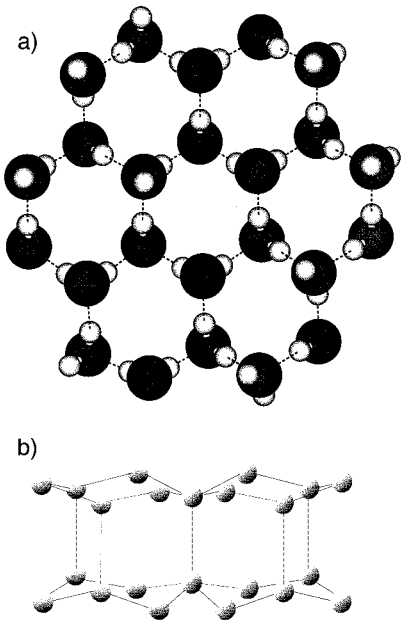


**Figure 1.** A top view (a) of the first bilayer of a basal plane ice surface (0001) equilibrated at $T_s = 10$ K. The dark atoms are the oxygen atoms of the water molecules and the light atoms are the hydrogen atoms. Panel b represents an illustration of the chairlike superimposed hexagonal rings in the first two bilayers (only oxygen atoms are shown).

## 3. Computational Results

The scattering plane of the ice surface (the first bilayer) at $T_s = 10$ K is shown in Figure 1a. In the scattering plane, the water molecules are arranged forming open hexagonal rings, providing a long-range symmetry, which is absent in the case of amorphous ice. The hexagonal rings have a chair-formed shape and are superimposed on each other (as illustrated in Figure 1b), forming shafts running perpendicular to the surface.

The computed sticking probability ($P_s$) of hydrogen atoms to the crystalline ice surface is presented in Figure 2 together with the previous classical trajectory results of Buch and Zhang[22] and Masuda et al.[42] for sticking of hydrogen to amorphous ice surfaces. Results are shown for two different surface temperatures, 10 and 70 K. Our calculations show that the sticking probability decreases rapidly with $E_i$ (Figure 2a). This trend agrees with the previous results for amorphous ice.[22,42] The reason that $P_s$ decreases with $E_i$ is that at higher $E_i$ more energy has to be transferred to the ice surface for trapping to occur. We find that the sticking probability at $T_s = 70$ K is significantly

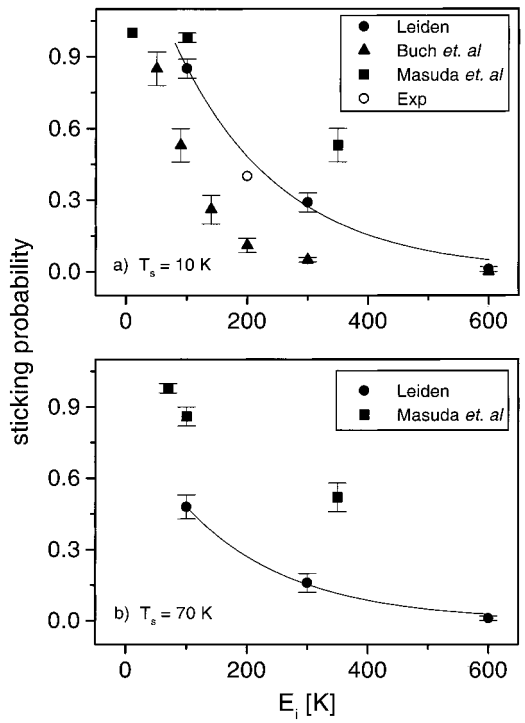


**Figure 2.** The sticking probability of hydrogen atoms to crystalline ice as a function of $E_i$ for (a) $T_s = 10$ K and (b) $T_s = 70$ K, together with the previous results on sticking of hydrogen to amorphous ice.[22,42] The solid line is an exponential decay fit of our results. An experimental data point for molecular hydrogen formation on amorphous ice is also shown at low $T_s$.[46] See the text for the connection of $H_2$ formation with the sticking of hydrogen atoms.

lower than at $T_s = 10$ K. This trend agrees qualitatively with the previous results for amorphous ice for low $E_i$ (100 K) (Figure 2b).[42] At higher surface temperatures, the water molecules are more dynamic and less packed. Energy transfer can also occur from the warm surface to the impinging atom, rather than the other way around (see below), leading to decreased adsorption of the impinging atom.

The sticking probabilities calculated here are lower than the values calculated by Masuda et al.,[42] but higher than those calculated by Buch and Zhang[22] (Figure 2). The recombination efficiency ($\gamma$) measured in beam experiments performed to study the formation of the molecular hydrogen on an amorphous ice surface at $T_s = 10$ K is also shown in Figure 2a.[46] The experiments showed that the recombination efficiency of $H_2$ on an amorphous ice surface not fully saturated with hydrogen atoms is about 0.4. The recombination efficiency can be defined as $\gamma = \eta P_s$,[16] where $\eta$ is the probability that a hydrogen adatom on the surface will recombine with another atom to form $H_2$. Assuming that $\eta = 1$, as was done by Pirronello et al.[11] in the comparison of their experimental data for $H_2$ formation on silicates to the model calculations of Hollenbach and Salpeter,[14] $P_s$ can be taken as 0.4 for the experimental conditions. The measured $P_s$ on amorphous ice is then in good agreement with the results of our calculations for crystalline ice, as shown in Figure 2a. The measured $\gamma \approx 0.4$ at $T_s = 10$ K is high enough for the formation of molecular hydrogen on ice surfaces to compete with the cosmic destruction of $H_2$.[39,46]

Our calculated sticking probability can be fitted with a simple exponential function:

$$P_s = \alpha\, e^{-E_i/\beta} \qquad (3.1)$$

where $\beta = 175$ K and $E_i$ is expressed in kelvin (1 K = 8.31 J/mol). The value of the preexponential factor $\alpha$ depends on $T_s$. We found $\alpha = 1.5$ for $T_s = 10$ K and $\alpha = 0.85$ for $T_s = 70$ K. Note that the fit expression is valid only for high enough $E_i$ such that $P_s < 1$. The calculated values of the sticking probability by Buch and Zhang ($S_E$ of Table 2 of ref 22) were fitted using eq 2 with $\alpha = 1$ and $\beta = 102$ K.[22] However, we could not fit the calculated data by Musada et al. using the decay function of eq 2, because too few data points were shown for high $E_i$.

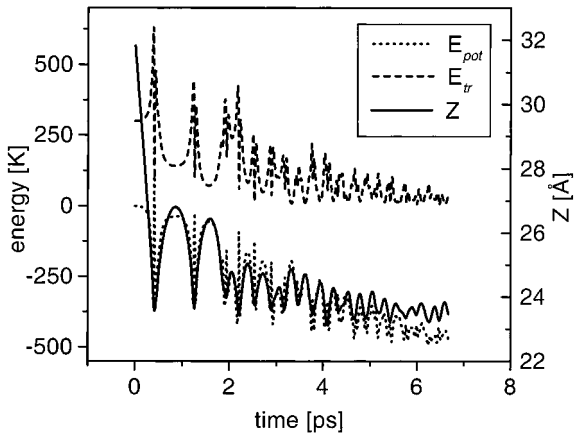


**Figure 3.** The translational and potential energies ($E_{tr}$ and $E_{pot}$, respectively) of the impinging atom and its $Z$ coordinate as a function of time for a typical sticking trajectory at $E_i = 300$ K and $T_s = 10$ K.

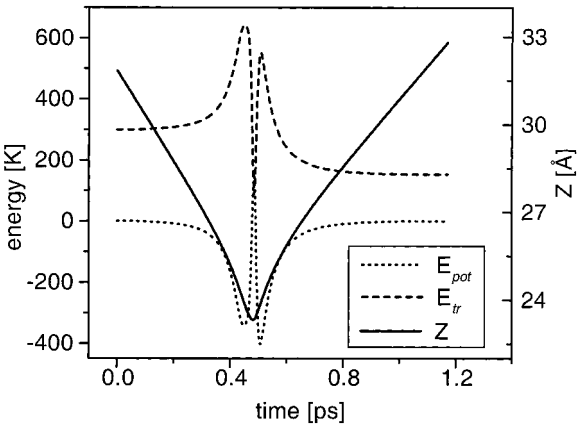


**Figure 4.** The translational and potential energies ($E_{tr}$ and $E_{pot}$, respectively) of the impinging atom and its $Z$ coordinate as a function of time for a typical backscattering trajectory at $E_i = 300$ K and $T_s = 10$ K.

We have monitored the kinetic and the potential energies of the impinging atom for most of the trajectories. For a typical sticking trajectory, the impinging atom is thermalized and trapped on ice after a few hops on the surface, as shown in Figure 3. The figure shows that the hydrogen atom loses its translational energy slowly via the collisions with the surface, indicating that the energy transfer to the ice surface is not efficient. This is a mass effect: the mass of the hydrogen atom is quite small compared to the mass of a water molecule (or several water molecules), obstructing efficient energy transfer from the impinging atom to the surface.[22]

For a typical backscattering trajectory, the hydrogen atom is scattered back after a single collision with the surface, retaining a significant amount of its translational energy (Figure 4). In some backscattering trajectories, a few collisions (up to six) with the ice surface are found to occur before the hydrogen atom is scattered to the gas phase. The same behavior was also observed in the calculations of Masuda et al.[42]

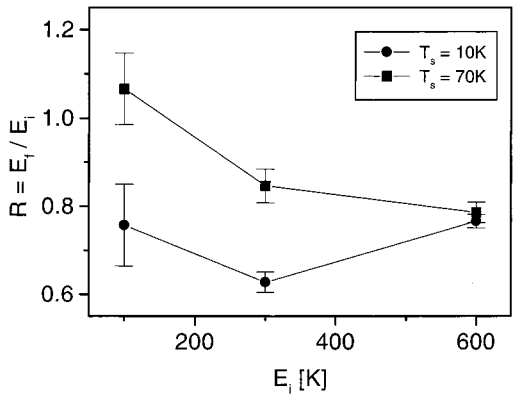


**Figure 5.** The ratio of the average final translational energy and $E_i$ as a function of $E_i$ for $T_s = 10$ and 70 K for backscattering trajectories.

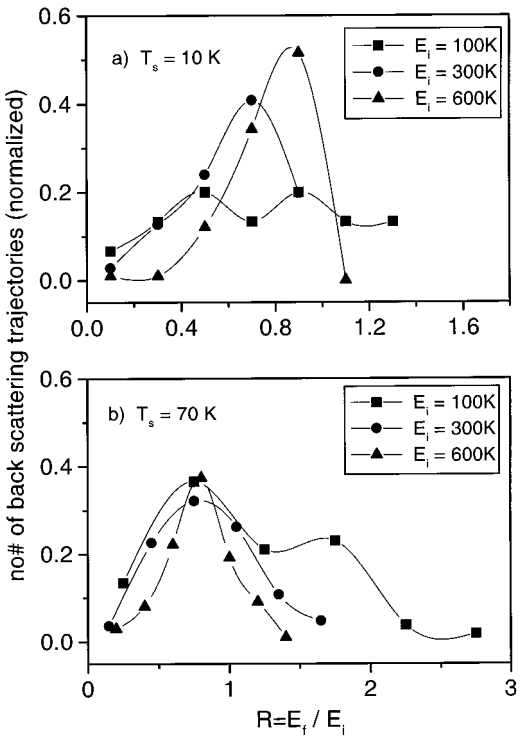


**Figure 6.** The final energy distributions at (a) $T_s = 10$ K and (b) $T_s = 70$ K for three values of $E_i$ for the case of backscattering.

In the case of backscattering, the hydrogen atom retains on average 70% of its initial translational energy, when scattered from the ice surface equilibrated at $T_s = 10$ K, as shown in Figure 5. At a higher surface temperature ($T_s = 70$ K), Figure 5 shows that the scattered hydrogen atom retains a larger amount of its initial translational energy: the figure shows the scattered atoms hitting the warm surface at $E_i = 100$ K even gain on average about 10% of their initial translational energy from the surface upon scattering. Thus, energy is transferred from the ice surface to the scattered hydrogen. Figure 6a,b shows the final energy distributions at $T_s = 10$ and 70 K, respectively, for the backscattering trajectories. At $T_s = 70$ K, the scattered atom may gain as much as its $E_i$. The distributions become sharper at higher values of $E_i$, at which the collisions with the surface become more elastic in nature. Note that for $E_i = 100$ K, a bimodal structure was observed in the distributions at both surface temperatures. This bimodality is not correlated with the number of bounces of the atom on the surface.

The adsorbed hydrogen atoms in most cases are found to be at about 1.0−2.0 Å above the ice surface (Figure 7). We have

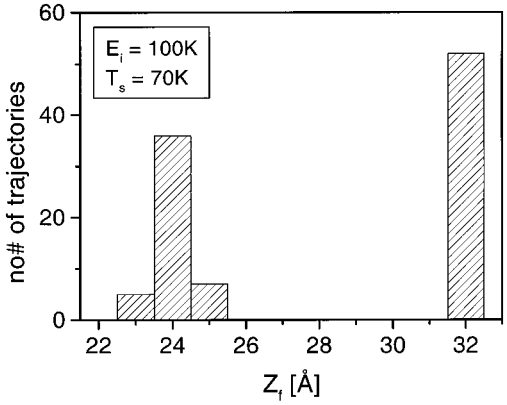


**Figure 7.** Histogram of the number of the trajectories distributed over the final value of the $Z$ coordinate for $E_i = 300$ K and $T_s = 70$ K. The surface is at 22.5 Å. The trajectories with $Z_f = 32.0$ are classified as backscattering trajectories; the rest are classified as sticking trajectories.

not seen any case of implantation (penetration); the interaction potential between a hydrogen atom and a single water molecule is a shallow potential (the "recommended" value of the spherically averaged potential depth is $\bar{\epsilon} \simeq 76$ K, which is much smaller than the energy of a hydrogen bond, which ranges from 1500 to 5000 K; of course, hydrogen bonds can only occur between N, O, and F, on one hand, and a "polar hydrogen atom" (covalently bonded to N, O, or F), on the other hand[60]), but it is also a strongly repulsive potential for $r \leq 2.5$ Å, which is about the distance from the center of a hexagonal ring to any water molecule belonging to the ring ($\bar{r}_{min} \approx 3.4$ Å).[22,57] Also, the collision energy in our calculations (up to 600 K $\simeq$ 5.0 kJ/mol) was quite low compared with the energy at which we first saw penetration of ice by HCl ($E_i \geq 96$ kJ/mol).[61] Calculations for a static ice lattice, similar to those performed to find the threshold value of $E_i$ for penetration of ice by HCl,[49] suggest that the hydrogen will be able to penetrate the surface of ice for $E_i \geq 96$ kJ/mol.

The average value of the final binding energy of the hydrogen atom at the end of a typical sticking trajectory is found to be around 400 ± 50 K (Figure 3). The value of the binding energy that we have found falls within the distribution of the minimum binding energies of the adsorbed H-atom on an amorphous ice cluster, which were calculated by Buch and Zhang (Figure 1 in ref 22) and is in good agreement with the results of the pioneering calculations.[14] Because of the properties of the potential energy surface of the H−$H_2O$ system, a small number of water molecules (five to six) is expected to contribute to the hydrogen−ice interaction. The top and side views of the final geometry of the system are shown for a typical adsorbing trajectory in Figure 8, parts a and b, respectively. The figures show that the hydrogen atom is adsorbed on top of the ice surface, at a distance of about 1.5 to 2.0 Å above the center of a water hexagonal ring. In this configuration, the hydrogen atom interacts with the six water molecules forming that ring at a distance of 3.0−3.5 Å from each water molecule. This configuration results in the binding energy of about 400 K that we have found.

## 4. Discussion

**4.1. Comparison to Computational Results for Amorphous Ice.** The amorphous ice cluster studied by Buch and Zhang[22] is a small cluster that consists of 115 water molecules. The cluster is irregular with many collision sites that consist of a small number of water molecules, which disfavor sticking because the attractive interaction between the hydrogen atom and the

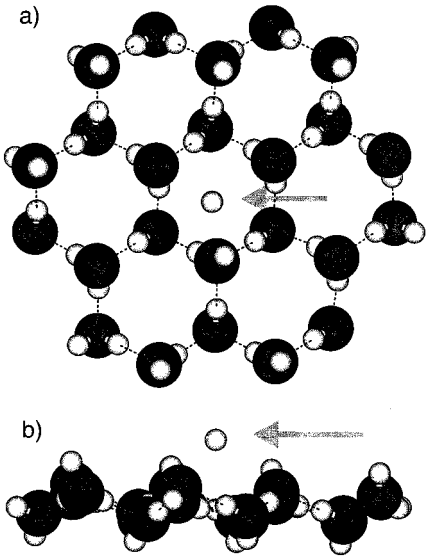


**Figure 8.** A top (a) and a side view (b) of the final configuration of a trapped hydrogen atom on the basal plane face of ice for a typical sticking trajectory. The arrows indicate the adsorbed hydrogen atom.

surface is weak at these sites. Therefore, a significant area of the ice lattice would not be suitable for adsorbing the incoming atom in the calculations of Buch and Zhang.[22] This explains why their sticking probability is generally lower than the sticking probability that we compute for crystalline ice at $T_s = 10$ K (Figure 2a).

On the other hand, Masuda et al.[42] modeled the amorphous ice surface with a larger number of water molecules (1000 water molecules), applying periodic boundary conditions to the directions parallel to the scattering plane. The nature of their amorphous ice is also different from our crystalline ice: in their case, the lack of symmetry and the presence of defects on the amorphous surface provide a broader distribution of the binding sites on the surface and hence a broader distribution of the binding energies compared to the case of the crystalline surface. In those calculations, the potential used to describe the water−water interaction is the pair potential, TIP2S,[52,62] the same potential as used by Buch and Zhang. Masuda et al. used the same $H_2O$−H potential as used by us and by Buch and Zhang. The calculations performed by Masuda et al. found, however, higher values of the sticking probability compared to our values and much higher values than those found by Buch and Zhang. Their calculations showed that the *maximum* binding energy of the adsorbed hydrogen atom is about 2000−2500 K (4−5 kcal/mol), which is a factor of 5 to 6 higher than our results and is comparable to the energy of a hydrogen bond. With the H−$H_2O$ potential used, such a large binding energy requires more than 30 water molecules to bind to the hydrogen atom at a distance of about 3.4 Å (because of the properties of the shallow potential that we have discussed). The *maximum* binding energy stated (2000−2500 K) was found when the hydrogen atom is about 1 Å below the level of the ice surface. Even in this configuration, the number of the water molecules interacting with the adsorbed atom at a distance of 3.4 Å would still be much smaller than 30. Also, in the calculations of Masuda et al., the *average* binding energy was found to be about 1250 K (2.5 kcal/mol),[42] which corresponds to the hydrogen atom interacting with more than 15 water molecules at a distance of about 3.5 Å from it.

The discrepancy between our results and the results of Masuda et al. is due to the use of an incorrect expression for the spherical harmonics, $Y_{00}$, in eq 2.1,[63] which was printed incorrectly in the paper in which the H−$H_2O$ interaction potential was presented[57] and also in the subsequent paper, in which the potential was used to study the interaction between H and D with an amorphous ice surface[22] ($Y_{00}$ was printed as $\sqrt{\pi/4}$ instead of $\sqrt{1/4\pi}$). The first term is the dominant term in equation (2.1), and the division of the maximum binding energy calculated by Masuda et al. by a factor of $\pi$ (to correct for the value of $Y_{00}$) should yield a *maximum* binding energy less than 800 K, which falls within the distribution of the binding energies of the adsorbed hydrogen atom shown in Figure 1 in ref 22. The corrected value of the *maximum* binding energy indicates that less than 12 water molecules interact with the adsorbed H-atom at a distance of 3.4 Å, which is a more realistic number for the configuration at which the adsorbed H-atom is 1 Å below the surface. Also, the corrected value for the *average* binding energy of the adsorbed hydrogen atom is $1250/\pi \approx 400$ K, in excellent agreement with our results. The corrected value of the *average* binding energy falls nicely within the binding energy distribution calculated by Buch and Zhang. Therefore, we conclude that the use of the incorrect expression for $Y_{oo}$ is responsible for the discrepancy between the results of Musada et al. and our results and those of Buch and Zhang.

**4.2. Astrophysical Implications.** In diffuse clouds, the $H_2$ formation is balanced by its dissociation by ultraviolet photons. The photodissociation of $H_2$ occurs through absorptions in the Lyman and Werner bands, followed by emission to the vibrational continuum.[64,65] The calculated destruction rate in the unattenuated radiation field is $5 \times 10^{-11}$ s$^{-1}$.[66] Because the grains in diffuse clouds do not have ice mantles until the extinction has reached at least 3 mag,[67] this $H_2$ destruction needs to be balanced by $H_2$ formation on bare silicate and carbonaceous grains rather than icy grains.

The situation considered in this paper is representative of dense clouds, in which the silicate grains have accreted an icy mantle. Here, the main destruction channel is cosmic-ray dissociation of $H_2$ at a rate of $\zeta \approx 2.6 \times 10^{-17}$ s$^{-1}$,[68] much less than the photodissociation rate in diffuse clouds. The main question here is not whether the cloud is largely molecular but what the remaining fraction of gas-phase atomic hydrogen is. These clouds have typical number densities of $n \approx 2n_{H_2} \approx 10^4$ cm$^{-3}$ and $T = 10$ K, where $n_{H_2}$ is the number density of $H_2$. An alternative situation is inside dense clouds close to sites of massive star formation. Here, both the density and temperature may be somewhat higher, $T = 100$ K and $n \approx 10^5$−$10^6$ cm$^{-3}$.

The corresponding rate of formation of $H_2$ per unit volume per unit time can be written as follows:[15,16]

$$K_F = Rn_H n = \frac{1}{2} n_H n_g \sigma_g v_H \gamma \qquad (4.1)$$

where $R$ is the rate constant of the $H_2$ formation on the grain surface, $n_H$ and $n_g$ are the number densities of hydrogen atoms and dust grains, $v_H$ is the average speed of the hydrogen atoms in the gas phase hitting a grain surface, and $\sigma_g$ is the average area of the cross section of a grain particle. The parameter $\gamma$ is the recombination efficiency. In the dense clouds, $n_g = 10^{-12} n = 10^{-8}$ cm$^{-3}$. The extinction observations show that $\sigma_g n_g \approx 2.1 \times 10^{-21} n$, where $n$ and $n_g$ are in cm$^{-3}$ and $\sigma_g$ is in cm$^{-2}$.[28] The average velocity of the hydrogen atoms in the gas phase hitting the surface can be written as $v_H = \sqrt{(\pi/2)(kT_{gas}/m)}$,[69] where $m$ is the atomic mass of the hydrogen atom. At $T_{gas} = 100$ K, $v_H$ equals $1.14 \times 10^5$ cm/s. The recombination efficiency $\gamma$ is set to equal the sticking probability. Then, for $T_s = 10$ K, $\gamma = 0.85$, and for $T_s = 70$ K, $\gamma = 0.3$. The rate constant $R$ calculated here is $1 \times 10^{-16}$ cm$^3$ s$^{-1}$ at $T_s = 10$ K and $3.6 \times 10^{-17}$ cm$^3$ s$^{-1}$ at $T_s = 70$ K for $n = 10^4$ cm$^{-3}$. In equilibrium,

the density of the hydrogen atoms $n_H = \zeta/R$.[28] The calculated $n_H$, $\sim$0.26 cm$^{-3}$ at $T_s = 10$ K and $\sim$0.72 cm$^{-3}$ at $T_s = 70$ K, is in reasonable agreement with the value calculated by Duley and Williams who found $n_H \approx 1$ cm$^{-3}$.[28] Our value for $R$ provides constraints on the amount of atomic hydrogen in the dense clouds, where $R$ is larger than $\zeta$. These calculations therefore suggest that the sticking of the hydrogen atoms and the subsequent formation of molecular hydrogen on ice surfaces could compensate the cosmic ray destruction of molecular hydrogen, as also concluded from the experimental results.[46]

## 5. Conclusions

We have presented results of classical trajectory calculations on sticking of hydrogen atoms to the basal plane face of crystalline ice. The calculations show a decrease of the sticking probability ($P_s$) with both $E_i$ and $T_s$. The sticking probability can be fitted with an exponential decay function, $P_s = 1.5\ e^{-E_i(K)/175}$ at $T_s = 10$ K and $P_s = 0.85\ e^{-E_i(K)/175}$ at $T_s = 70$ K. Hopefully, the dependence of $P_s$ on $E_i$ and $T_s$ predicted here can be confirmed experimentally.

In the case of adsorption, the hydrogen atom ends up trapped on top of the center of a water hexagonal ring at a distance of about 1.5 Å from the ice surface. In this configuration, the trapped atom interacts with the six water molecules of that ring. The binding energy of the trapped hydrogen atom is found to be $400 \pm 50$ K, a value which falls within the binding energy distribution of the hydrogen atoms adsorbed on amorphous ice as calculated by Buch and Zhang.[22] In most backscattering trajectories, the hydrogen atom is scattered to the gas phase after a few collisions with the ice surface.

Our results show that the energy transfer from the hydrogen atom to the surface is not efficient, in contrast to the case of HCl colliding with an ice surface at hyperthermal energies.[49] This is partly due to a mass effect: the mass of the hydrogen atom is quite small compared to the mass of the water molecule, in contrast to the HCl−ice case. The scattered hydrogen atom retains a significant amount of its initial translational energy ($\langle E_f \rangle$ is about 70% of $E_i$ at $T_s = 10$ K and about 90% at $T_s = 70$ K).

Discrepancies between our results for crystalline ice and those on sticking of hydrogen to amorphous ice of Buch and Zhang can be attributed to differences in surface topology.[22] We find that an incorrect use of the expression of the interaction potential between the water molecule and the hydrogen atom in the calculations of Masuda et al.[42] is responsible for the large discrepancy with their results.

The results of our calculations agree with the beam experimental data obtained by Manico et al.,[46] under the assumption that all H-atoms that stick also react. Our results on the efficiency of $H_2$ formation provide constraints on the amount of atomic hydrogen left inside the dense clouds, in agreement with the conclusions arrived at in the experiments of Manico et al.[46]

**Acknowledgment.** This research is part of the program of FOM and is financially supported by NWO. We acknowledge allocations of computer time by the National Computing Facilities foundation (NCF).

## References and Notes

(1) van Dishoeck, E. F. In *The Molecular Astrophysics of Stars and Galaxies*; Hartquist, T. W., Williams, D. A., Eds.; Clarendon Press: Oxford, U.K., 1998; p 53.

(2) Ehrenfreund, P.; Schutte, W. A. In *Astrochemistry: From Molecular Clouds to Planetary Systems: Proceedings of the 197th symposium of the International Astronomical Union held in Sogwipo, Cheju, Korea, 23−27 August 1999*; Minh, Y. C., van Dishoeck E. F., Eds.; International Astronomical Union by Astronomical Society of the Pacific: San Francisco, CA, 2000; Vol, 197, p 135.

(3) Hagen, W.; Tielens, A. G. G. M.; Greenberg, J. M. *Chem. Phys.* **1981**, *56*, 367.

(4) Moore, M. H.; Ferrante, R. F.; Hudson, R. L.; Nuth, J. A., III; Donn, B. *Astrophys. J.* **1994**, *428*, L81.

(5) Maldoni, M. M.; Robinson, G.; Smith, R. G.; Duley, W. W. *Mon. Not. R. Astron. Soc.* **1999**, *309*, 325.

(6) Chakarov, D.; Kasemo, B. *Phys. Rev. Lett.* **1998**, *81*, 5181.

(7) van de Hulst, H. C. *Rech. Astron. Obs. Part II.;* **1943**, *Utrecht XI*.

(8) King, A. B.; Wise, H. *J. Phys. Chem.* **1963**, *67*, 1163.

(9) Schutte, A.; Bassi, D.; Tommasini, F.; Turelli, F.; Scoles, G.; Herman, L. J. F. *J. Chem. Phys.* **1976**, *64*, 4135.

(10) Pirronello, V.; Liu, C.; Shen, L.; Vidali, G. *Astrophys. J.* **1997**, *475*, L69.

(11) Pirronello, V.; Biham, O.; Liu, C.; Shen, L.; Vidali, G. *Astrophys. J.* **1997**, *483*.

(12) Gould, R. J.; Salpeter, E. E. *Astrophys. J.* **1963**, *138*, 393.

(13) Williams, D. A. *Astrophys. J.* **1968**, *151*, 935.

(14) Hollenbach, D.; Salpeter, E. E. *J. Chem. Phys.* **1970**, *53*, 79.

(15) Hollenbach, D.; Salpeter, E. E. *Astrophys. J.* **1971**, *163*, 155.

(16) Hollenbach, D. J.; Werner, M. W.; Salpeter, E. E. *Astrophys. J* **1971**, *163*, 165.

(17) Lee, T. J. *Nature* **1972**, *273*, 99.

(18) Goodman, F. O. *Astrophys. J.* **1978**, *226*, 87.

(19) Smoluchowski, R. *J. Phys. Chem.* **1983**, *87*, 4229.

(20) Leitch-Devlin, M. A.; Williams, D. A. *Mon. Not. R. Astron. Soc.* **1984**, *210*, 577.

(21) Pirronello, V.; Averna, D. *Astron. Astrophys.* **1988**, *196*, 201.

(22) Buch, V.; Zhang, Q. *Astrophys. J.* **1991**, *379*, 647.

(23) Duley, W. W. *Mon. Not. R. Astron. Soc.* **1996**, *279*, 591.

(24) Shalabiea, O. M.; Caselli, P.; Herbst, E. *Astrophys. J.* **1998**, *502*, 422.

(25) Takahashi, J.; Masuda, K.; Nagaoka, M. *Mon. Not. R. Astron. Soc.* **1999**, *306*, 22.

(26) Parneix, P.; Brechignac, P. *Astron. Astrophys.* **1998**, *334*, 363.

(27) Farebrother, A. J.; Meijer, A. J. H. M.; Clary, D. C.; Fisher, A. J. *Chem. Phys. Lett* **2000**, *319*, 303.

(28) Duley, W. W.; Williams, D. A. *Interstellar Chemistry*; Academic Press: London, 1984.

(29) Hunter, D. A.; Watson, W. D. *Astrophys. J.* **1978**, *226*.

(30) Williams, D. A. In *Dust and Chemistry in Astronomy*; Millar, T. J., Williams, D. A., Eds.; IOP Publishing: Bristol, U.K., 1993; p 143.

(31) Herbst, E. *Annu. Rev. Phys. Chem.* **1995**, *46*, 27.

(32) Eley, D. D.; Rideal, E. K. *Nature* **1940**, *146*, 401.

(33) Eley, D. D. *Proc. R. Soc. London* **1941**, *178*, 452.

(34) Langmuir, I. *Trans. Faraday Soc.* **1922**, *17*, 621.

(35) Hinshelwood, C. N. *Ann. Res. London Chem. Soc.* **1930**, *27*, 11.

(36) Williams, D. A. In *Physical Processes in Instellar Clouds*; Morfill, E., Scholer, M., Eds.; D. Reidel Publishing Company: Dordrecht, Netherlands, 1987; p 377.

(37) Lennard-Jones, J. E.; Devonshire, A. F. *Nature* **1936**, *137*, 1069.

(38) Katz, N.; Furman, I.; Biham, O.; Pirronello, V.; Vidali, G. *Astrophys. J.* **1999**, *522*, 305.

(39) Biham, O.; Furman, I.; Katz, N.; Pirronello, V.; Vidali, G. *Mon. Not. R. Astron. Soc.* **1998**, *296*, 869.

(40) Biham, O.; Furman, I.; Pirronello, V.; Vidali, G. *Astrophys. J.* **2001**, *553*, 595.

(41) Aronowitz, S.; Chang, S. *Astrophys. J.* **1985**, *293*, 243.

(42) Masuda, K.; Takahashi, J.; Mukai, T. *Astron. Astrophys.* **1998**, *330*, 773.

(43) Takahashi, J. *Earth, Planets Space* **1999**, *51*, 1215.

(44) Meijer, A. J. H. M.; Farebrother, A. J.; Clary, D. C.; Fisher, A. J. *J. Phys. Chem. A* **2001**, *105*, 2173.

(45) Pirronello, V.; Liu, C.; Shen, L.; Vidali, G. *Astron. Astrophys.* **1999**, *344*, 681.

(46) Manico, G.; Raguni, G.; Pirronello, V.; Roser, J. E.; Vidali, G. *Astrophys. J.* **2001**, *548*, L253.

(47) Porter, R. N.; Raff, L. M. *Dynamics of Molecular Collisions, Part B;* Plenum: New York, 1976.

(48) Kroes, G. J.; Clary, D. C. *J. Phys. Chem.* **1992**, *96*, 7079.

(49) Al-Halabi, A.; Kleyn, A. W.; Kroes, G. J. *J. Chem. Phys.* **2001**, *115*, 482.

(50) Allen, M. P.; Tildesley, D. J. *Computer Simulations of Liquids*; Clarendon: Oxford, U.K. 1987.

(51) Bernal, J. D.; Fowler, R. H. *J. Chem. Phys.* **1936**, *1*, 515.

(52) Jorgensen, W. L.; Chandrasekhar, J.; Madura, J. D.; Impey, R. W.; Klein, M. L. *J. Chem. Phys.* **1983**, *79*, 926.

(53) Kroes, G. J. *Surf. Sci.* **1992**, *275*, 365.

(54) Karim, O. A.; Haymet, A. D. J. *J. Chem. Phys.* **1988**, *89*, 6889.

(55) Berendsen, H. J. C.; Postma, J. P. M.; van Gunsteren, W. F.; Dinola, A.; Haak, J. R. *J. Chem. Phys.* **1984**, *81*, 3684.
(56) Fincham, D. *Mol. Simul.* **1992**, *8*, 165.
(57) Zhang, Q.; Sabelli, N.; Buch, V. *J. Chem. Phys.* **1991**, *95*, 1080.
(58) Boys, S. F.; Bernardi, F. *Mol. Phys.* **1970**, *19*, 553.
(59) Bassi, D.; Paz, M. D.; Pesce, A.; Tommasini, F. *Chem. Phys. Lett.* **1974**, *26*, 422.
(60) Eğe, S. *Organic Chemistry*; Houghton Mifflin Company: New York, 1999.
(61) Al-Halabi, A.; Kleyn, A. W.; Kroes, G. J. *Chem. Phys. Lett.* **1999**, *307*, 505.
(62) Jorgensen, W. L. *J. Chem. Phys.* **1982**, *77*, 4156.
(63) Takahashi, J. Private communication.
(64) Stecher, T. P.; Williams, D. A. *Astrophys. J. Lett.* **1967**, *149*, L29.
(65) Dalgarno, A.; Stephens, T. L. *Atsrophys. J. Lett.* **1970**, *160*, L107.
(66) Black, J. H.; Dishoek, E. F. V. *Astrophys. J.* **1987**, *322*, 412.
(67) Whittet, D. C. B. *Dust in the Galactic Environment*; IOP Publishing: Bristol, U.K., 1992.
(68) van der Tak, F. F. S.; van Dishoeck, E. F. *Astron. Astrophys.* **2000**, *358*, L79.
(69) Greiner, W.; Neise, L.; Stocker, H. *Thermodynamics and Statistical Mechanincs*; Springer-Verlag: New York, 1997.